

Modal Identification of Lightly-Damped, Highly-Symmetric Bladed Disks

S.J. DiMaggio* and Z.H. Duron†

The Aerospace Corporation, P.O. Box 92957, Los Angeles, CA 90009-2957

G. Davis‡

The Boeing Company, Rocketdyne Propulsion & Power, P.O. Box 7922, Canoga Park, CA 91309-7922

Abstract

Turbine blade cracking or failure due to high-cycle fatigue is a concern in both aerospace and aircraft engines. Due to manufacturing advances leading to integrally-bladed disks, non-uniformities and damping associated with the blade-to-disk interface have been considerably reduced. In systems such as these, bladed-disk assemblies can behave as lightly-damped, rotationally-periodic structures in which many resonant conditions, involving response in all of the blades, exist. Due to the non-uniform, aerodynamic forces on the blades, excessive vibration response in the high-frequency regime can be a problem and, thus, identification of resonant conditions in this region of the spectrum is important in avoiding operation at potentially damaging speeds. Additionally, recent advances in computational methods have allowed bladed-disk assemblies to be treated numerically, albeit with complex models containing many degrees of freedom. This paper presents a modal identification technique that can help locate potentially harmful resonant conditions and aid in the validation of computational models of highly-tuned, bladed-disk assemblies across a wide frequency regime. An example is presented using data acquired from an impulse test of a turbine and includes results up to 20 kHz.

Nomenclature

b	given number of blades
f	frequency, Hz
f_n	natural frequency, Hz
FRF	frequency response function
$H_{i,j}$	FRF relating response at blade i to impact at blade j , g/lbf
H_{ref}	FRF of reference blade, g/lbf
i	blade number

j	number of nodal diameters in mode
\hat{n}	number of nodal diameters for given mode
n_b	number of nodal diameters in b blades
t	time, s
t_{ref}	reference time, s
TPA	turbopump assembly
y_i	modal amplitude of blade i
y_{ref}	modal amplitude of reference blade
$\phi_{i,j}$	phase relating response at blade i to impact at blade j
ϕ_{ref}	phase of reference blade, rad
θ_i	angular position of blade i , rad

Introduction

Prevention of high-cycle fatigue failures, induced by resonant vibration, in turbines is critical in the aerospace, aircraft and power industries. It is not surprising, therefore, that an extensive amount of research has been directed at understanding and accurately predicting the vibration characteristics of turbine blading.¹⁻⁷ Much of this knowledge is derived from analytical models that vary in their ability to treat mistune conditions and their applicability to predicting response in the high-frequency regime. Regardless of the particular methodologies used, however, the complexity of bladed disk, or blisk, systems suggests that experimental methods be used to verify and validate the theoretical predictions.

This paper presents an expedient (from a test time and post-processing standpoint) mode extraction method that can be used across a wide frequency range and requires information that can be acquired using a minimal amount of instrumentation. It is suggested that a single accelerometer, an instrumented force hammer and a dual-channel data acquisition

* Project Leader, Environmental Test & Ordnance Department, Member AIAA

† Senior MTS, Structural Dynamics Department, Member AIAA

‡ Senior Engineering Specialist, Development Stress/Advanced Analysis

Copyright © 2002 by The Aerospace Corporation. Published by the AIAA, Inc., with permission.

system are all that is needed in order to conduct impulse response tests from which modal information can be extracted and used to validate complex numerical models and/or Campbell diagrams. In fact, for the high sampling rates required in the example problem described in a later section of this paper, the data acquisition system could only acquire two channels of data simultaneously. Reference 8 provides a thorough explanation of the impulse testing employed to obtain the data required for the modal identification approach documented herein. The experimental technique presented requires an understanding of the well-documented behavior of rotationally-periodic structures and requires that the blisk be highly-tuned and the modes be well-separated. While these restrictions may initially seem rather limiting, the introduction of integrally-bladed disks with minimal damping and mistuning, in both aerospace and aircraft turbines, seems to make the approach attractive.

The accurate extraction of modal characteristics for highly-tuned blisks presents many challenges, chief of which is the sensitivity of the structure to perturbations due to the measurement system. This problem, discussed in Ref. 9, has led most experimentalists to employ relatively non-obtrusive measurement schemes, including laser vibrometers,^{9,10} strain gauges,¹¹ fiber optic sensors¹² and proximity probes.¹³ Additional experimental approaches related to turbines are also discussed in the context of accurately measuring blisk damping values.¹⁴⁻¹⁶ Nevertheless, a systematic approach to experimental verification of complex blisk models is not well established.

Since the experimental techniques discussed herein are aimed at validation of computational models and, at the same time require, *a priori*, an understanding of blisk vibration response developed using early theoretical analyses, a brief review of the previous numerical work is given here. While early computational approaches entailed beam, plate and finite element models of a cantilevered blade,¹⁷⁻²⁰ advances in computer technology have led to attempts at modeling entire blisk assemblies. Even with the advances in computing power, however, the costs of analyzing complete assemblies using traditional finite element approaches remain high. Two application-specific numerical approaches have been investigated by other researchers and show promise in mitigating the computational constraints associated with analysis of entire blisk assemblies. Using substructuring techniques, a full system model can be constructed using finite element representations of the disk (without blades) and a single blade by coupling the individual models at the disk-blade interface degrees-of-

freedom.²¹⁻²³ Other researchers use cyclic-symmetry assumptions in order to model an entire assembly by considering only a portion, or substructure, of the blisk with appropriate, complex boundary conditions.²⁴⁻²⁶ These models are useful for highly-tuned blisks, in which negligible blade-to-blade variability exists. Regardless of the approach, the adequacy of the results depends on the assembly of the individual components into the full system model and, consequently, appropriate experimental confirmation of the resulting predictions, using modal testing techniques, is necessary.

Background

A blisk and shaft are illustrated in Fig. 1, supported on a special stand used during the tests. As a result of a unique design and manufacturing process, the structural system illustrated in Fig. 1 exhibits extremely low damping and is highly redundant. For example, structural damping values on the order of 0.01% of critical were measured. The term “highly redundant” implies that blade-to-blade variability in material and geometric properties can be considered negligible. This symmetry led to attempts to numerically model the system using deterministic analyses in which all of the blades have exactly the same properties. In support of these analyses, experiments described in detail in Ref. 8 were conducted and system identification procedures, to be described herein, were developed to support the verification and validation of these models. “Mistuned” system behavior,^{27,28} resulting from even a small degree of blade-to-blade variability, cannot be predicted using simplified analytical models that assume rotational periodicity, and statistical techniques become necessary.

In the case of the tuned turbine rotor, the blade modes of vibration occur in families, or clusters, that are described according to their relationship to responses of a single blade mounted (cantilevered) on a rigid base or, in other words, uncoupled from the disk. For instance, at any particular resonant frequency in which the blades deform relative to the disk, the blades exhibit a response shape characteristic of one of the modes of a single, cantilevered blade. All blades around the circumference of the disk, however, do not deform with the same modal amplitude or phase. Rather, the amplitude and phase vary in a periodic manner around the circumference of the disk with a given number of nodal diameters. For a given single, cantilevered-blade mode shape, the number of nodal diameters in the coupled-system mode governs

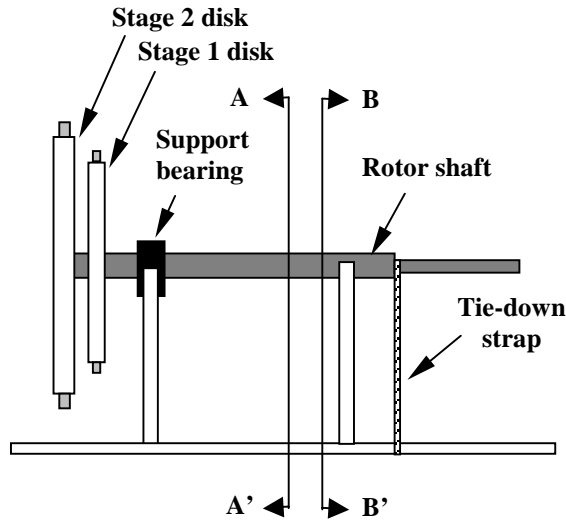


Fig. 1 Turbopump blisk and shaft supported in test stand. Stage 1 blades (smaller) and stage 2 (larger) blades are shown at the left end of the blisk assembly. Note the bearing that is seated in the left-hand support.

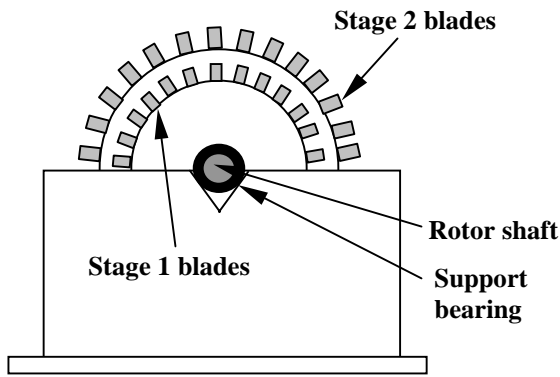


Fig. 1a Section A-A'.

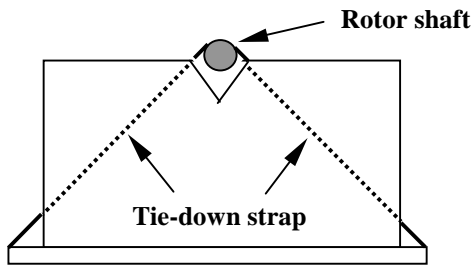


Fig. 1b Section B-B'.

the amplitude and phase relationship between individual blades on the rim. The total number of nodal-diameter manifestations, or diametrals, of each single, cantilevered-blade mode is $m = (N - 1) / 2$, for N odd, where N is the number of blades.

For the turbine rotor tested, 123 stage-one blades were present; resulting in 61 diametrals for each of the single, cantilevered-blade mode shapes. For a tuned blisk, vibrating in a mode having j nodal diameters, the modal amplitude of blade i on the periphery can be expressed as⁷

$$y_i = A \sin(j\theta_i) \cos(2\pi f_n t), \quad (1)$$

for

$$\theta_i = \frac{2\pi}{123}(i-1), \quad i = 1, \dots, 123, \quad (2)$$

as shown in Fig. 2. The shape of vibration on the periphery of the disk is $A \sin j\theta_i$, while the frequency of the resonant oscillation is denoted f_n .

The drawings in Fig. 2 are intended to illustrate modal response for the first three diametrals. For the first diametral, a single nodal-diameter line exists, and the two blade groups located on either side of this node line respond with opposite phase. Although this may be the first diametral, the blade response relative to the disk can be characterized by any of the mode shapes for a single, cantilevered blade. If blades are located exactly on the nodal diameter line, however, they exhibit no response. For a diametral characterized by j nodal diameter lines, blades located exactly $\phi = 2\pi / j$ radians apart, exhibit the same amplitude- and phase-response behavior. For

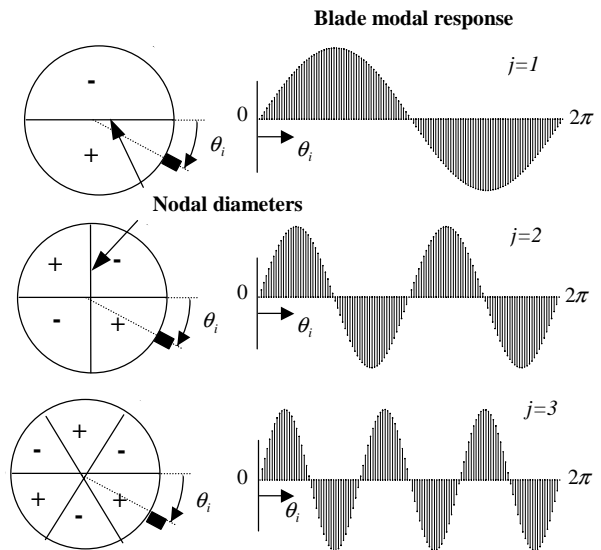


Fig. 2 Vibration modes of a highly tuned bladed disk.

example, the second diametral corresponds to $j = 2$ and, as shown in Fig. 2, blades separated by $\phi = \pi$ radians exhibit the same amplitude and phase response. As the number of nodal diameters increases, the natural frequencies of the coupled system, or blisk, asymptotically approach their respective cantilevered frequencies of a single blade.

The nomenclature used in this report is introduced by considering what is referred to as the eighth diametral of the third blade mode. This mode shape is denoted as 3(8) and describes a mode characterized by blades that deform relative to the disk in the third cantilevered mode shape. In this mode, the response amplitude and phase of individual blades vary sinusoidally around the blisk circumference with eight full waves.

In the following sections of this paper, it is assumed that high-quality FRFs, relating the acceleration response at blade number one to a force input at blades one through 24, for frequencies up to 20 kHz, have been acquired. For a detailed explanation of the experimental techniques required to obtain these responses, the reader is referred to Ref. 8.

FRFs for Single Blade Test Article

Prior to testing the complete blisk assembly illustrated in Fig. 1, a single-blade article, mounted on a flexible base, was tested. See Ref. 8 for details. This preliminary test provided the experimentalist a reasonable expectation of where in the frequency spectrum modal clusters associated with each cantilevered-blade mode would exist. This test was also used to verify the single blade analytical model that, using component-mode synthesis, was assembled into the complete, numerical blisk model.

The single-blade FRF magnitude estimate, relating acceleration response to the applied impulsive force, is shown in Fig. 3. The first three resonant peaks for the single-blade test article are easily identified at

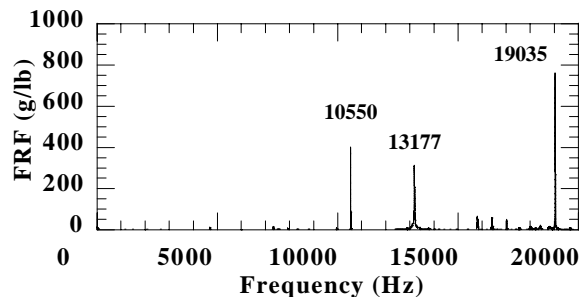


Fig. 3 FRF Magnitude for single blade test article.

10550, 13177 and 19035 Hz, respectively. A finite element model was also generated for the single-blade test article, and the computed natural frequencies (for the first three modes) show good correlation with the experimental results, as shown in Table 1. The results of the numerical model for the single blade, with the flexible base removed and a cantilevered boundary condition imposed, are also shown in the table.

Table 1. Summary of Single Blade Frequencies

Mode	Experimental Results	Numerical Model Flexible Base	Numerical Model Cantilevered
	1	10550	10551
2	13177	13181	14442
3	19035	19000	21176

FRFs for Complete Blisk

The FRF shown in Fig. 4 was determined from the full-blisk tests and relates acceleration response at blade 1 due to an impulse applied to blade 1. Blade measurement locations (for both impact and response) were the same as those employed during the single-blade tests.

Comparison of the FRF magnitude in Fig. 4 with the single-blade results, shown in Fig. 3, reveals significant differences in spectral character. Whereas the single-blade FRF magnitude contains three dominant resonances, associated with blade bending and torsional behavior, the strong coupling between the blades on the blisk rim leads to the appearance of many closely-spaced resonances in the full-blisk system. The FRF magnitude in Fig. 4 is characterized by the presence of three clusters, or families, of blade modes. In each cluster, the blade-mode diametrals are observed to asymptotically approach frequencies of 10335 Hz, 13408 Hz, and 19595 Hz, respectively. As expected, these frequencies are all below the cantilevered frequencies summarized in Table 1.

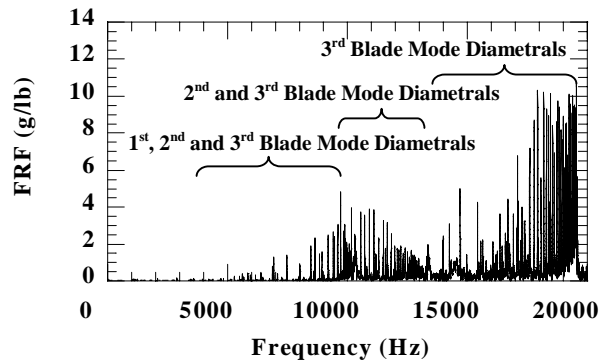


Fig. 4 FRF Magnitude relating blisk response at blade 1 to impulse applied at blade 1.

Figure 5 shows an expanded view of the region between 12 and 13 kHz in Fig. 4. From the information in Table 1 and an understanding of the well-documented behavior of highly-tuned bladed disks, the probable mode shapes associated with the resonant peaks shown in Fig. 5 can be inferred. As indicated in Fig. 4, the resonant peaks associated with the higher-order, cantilevered-blade modes can be interspersed with the lower-order, cantilevered mode shapes. For example, while the closely spaced peaks at 12772 Hz and 12786 Hz might, in other structural systems, be interpreted as a split second mode resonance, mode-extraction techniques reveal the 12772 resonance to be the eighth diametral of the third blade mode. Conversely, none of the first blade-mode diametrals exist above the associated cantilever frequency of 11868 Hz and, thus, are not evident in Fig. 5.

Mode Extraction

Blisk mode shape information is readily derived from measured FRFs that relate response (output) at each blade to a single impact (input). The FRFs acquired during test related the response at blade 1 (reference measurement location) to impacts applied sequentially to each blade tested. Maxwell's Reciprocal Theorem* suggests that the FRFs relating acceleration response at blade 1 to impulses applied at blades $j = 1, \dots, 24$ can be considered to be identical to FRFs relating the acceleration at blades $i = 1, \dots, 24$ to an impulse applied at blade 1. With this result, blisk mode shapes can be identified on the basis of the measured FRFs and the assumed sinusoidal character of blade response at a single resonant frequency.

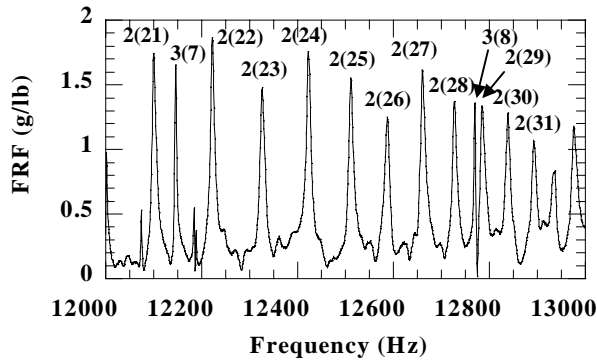


Fig. 5 Expanded view of Fig. 4.

* Applying Maxwell's Reciprocal Theorem to this test procedure implies that the response at blade i due to a force applied at blade j is equal to the response at blade j due to a force applied at blade i .

For an arbitrary time t and a given frequency f , the response at each blade tested, due to an impulse applied at blade 1, is expressed by

$$y_i(t, f) = |H_{i,1}(f)| \sin[2\pi f t + \phi_{i,1}(f)], \quad (3)$$

where $|H_{i,1}(f)|$ and $\phi_{i,1}(f)$ are the FRF magnitude and phase of the response at blade $i = 1, \dots, 24$, due to an impulse at blade 1. By virtue of Maxwell's Theorem, these quantities are equivalent to the measured FRF magnitude and phase, $|H_{1,i}(f)|$ and $\phi_{1,i}(f)$, acquired by measuring the response at blade 1 due to impulses applied sequentially to blades one through 24.

Of the 24 blades tested, any one of them may be arbitrarily selected so that its estimated modal response amplitude is equal to its FRF magnitude estimate. For a particular resonant frequency, f_n , this location is taken as the reference location, where

$$y_{ref}(f_n) = |H_{ref}(f_n)| \quad (4)$$

and

$$\sin[2\pi f_n t + \phi_{ref}(f_n)] = 1. \quad (5)$$

By virtue of Eq. (5), this response occurs at the arbitrary time

$$t = t_{ref} = \frac{1}{2\pi f_n} \left(\frac{\pi}{2} - \phi_{ref} \right). \quad (6)$$

The responses of all other blades can now be synchronized in time by setting $t = t_{ref}$ in Eq. (3), and their resulting modal response estimates are computed as

$$y_i(t_{ref}, f_n) = |H_{1,i}(f_n)| \sin[2\pi f_n t_{ref} + \phi_{1,i}(f_n)] \quad (7)$$

While the ratios of these modal amplitudes characterize the unique shape of the modal response, their amplitudes can be scaled by any factor necessary for visualization. In the case of these tests, a scale factor of 50 was used to obtain the modal plots contained herein.

Using this procedure, response shapes associated with the blade resonances at 12728 Hz, 12772 Hz, and at 12786 Hz were identified and are shown in

Fig. 6. In each of the plots shown, the x-axis indicates the blade numbers from 1 to 24, while the y-axis indicates the corresponding modal amplitudes, $y_i(t_{ref}, f_n)$. Computed blade modal amplitudes are denoted by the solid dots connected by straight solid lines, and a “smoother” result, obtained through a spline fit, is also shown. In both cases, however, the nature of the mode shape is preserved, and the periodic pattern is what an observer would see at a single instant of time, in the plane of the disk, if the circumference were “unwrapped,” or laid out in a straight line. Uniformly high coherence values, associated with the FRF estimates (at the particular frequency under consideration) for each individual blade, are denoted by diamonds connected by solid lines.

Since these mode-shape plots contain information for the first 24 blades only, a determination of the number of nodal diameters for the entire disk is obtained by

$$\hat{n} = \frac{123n_b}{b}, \quad (8)$$

where \hat{n} is the number of nodal diameters present in the entire disk and n_b is the number of nodal diameters observed in b blades. The ratio n_b/b is the number of nodal diameters-per-blade which, when multiplied by 123 (total number of stage-one blades), yields the number of nodal diameters present in the blisk. In this manner, the number of blisk nodal diameters can be identified from responses acquired over a portion of the blisk. For example, in Fig. 6(a), using the smoothed mode shape curve, $n_b=4$ nodal diameters were observed over $b=(20.4-3)=17.4$ blades yielding $\hat{n}=(4 \times 123)/(20.4-3)=28.3$ or, approximately, 28 diametrals present in the entire disk. Similar calculations are also shown in Fig. 6(b) and (c) for the 3(8) and 2(29) modes. Note that the smoothed curve was used in order to obtain a fractional number of blades b , rather than simply using the integer number of blades in the physical system. This allowed the resonant peaks at 12728, 12772, and 12786 Hz (shown in Fig. 5) to be identified as the 2(28), 3(8) and 2(29) modes of the blisk. Recall that the nomenclature 2(28) indicates that the mode is characterized by blade deformation relative to the disk in the second cantilevered mode, with an amplitude and phase variation, around the circumference of the disk, characterized by 28 nodal diameters, or full waves.

Examination of the FRF curve in Fig. 5 reveals a pattern in which the spacing between the majority of

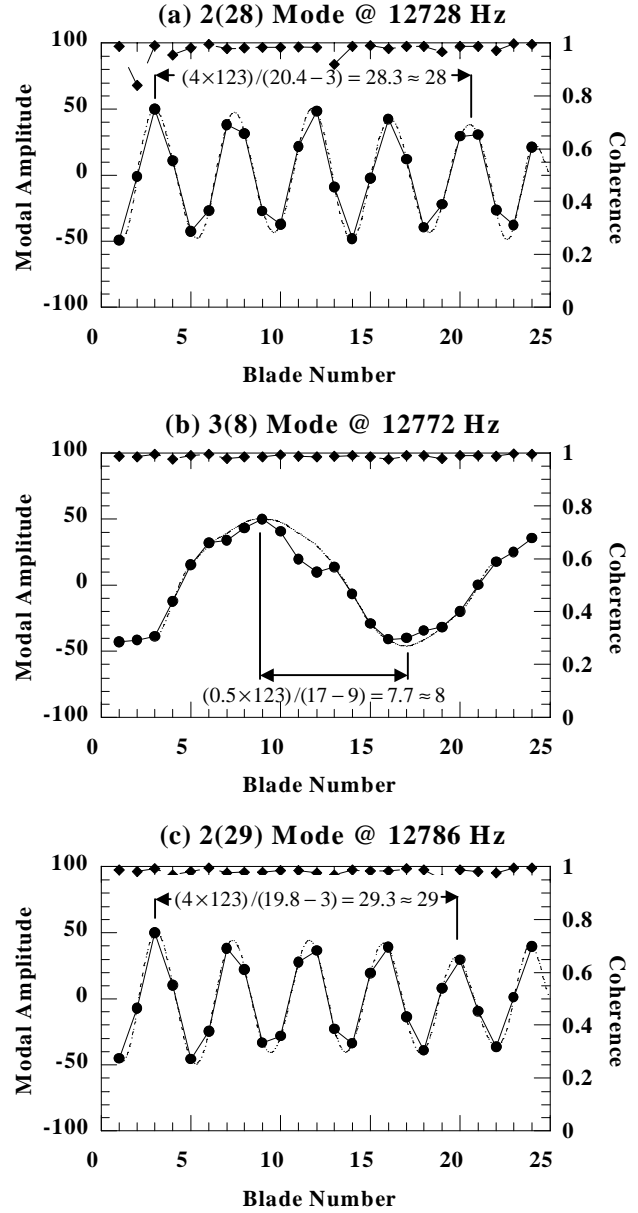


Fig. 6 Response shapes corresponding to 2(28), 3(8) and 2(29) modes.

resonant peaks appears to decrease with increasing frequency. This is characteristic of the fact that the natural frequencies of the second blade-mode family asymptotically approach the associated cantilever frequency, estimated by the single-blade, cantilevered model to be 14442 Hz. Identifying the number of diametrals associated with a single resonant peak in the family, therefore, is often sufficient to infer the number of nodal diameters associated with the remaining resonances. For example, if the mode extraction process identifies the 2(24) and 2(28) modes in Fig. 5, it is reasonable to infer that the three interme-

diate peaks correspond to the 2(25), 2(26) and 2(27) modes. An exception in the Fig. 5 trend is the response at 12772 Hz, which was presumed to be a diametral associated with the third blade-mode family on the basis of an initial visual inspection of the FRF. By virtue of the response shape shown in Fig. 6(b), this resonant peak was subsequently determined to be the 3(8) blade mode. Closer examination of the FRF over a wider frequency range indicates that the response at 12772 Hz, while being interspersed with second mode diametrals, does fall into a similarly ordered numerical pattern that characterizes the third blade mode family.

Identification of blade modal responses using Eqs. (3)-(7) has been shown to yield reasonable estimates of mode shapes for applications where the measured FRFs are characterized by well-spaced resonant behavior. For example, the FRF magnitude in Fig. 5 shows a resonance at 12728 Hz that is fairly well-isolated from neighboring peaks, while the response at 12772 Hz, however, is influenced by the peak at 12786 Hz. This coupling manifests itself in the corresponding mode shape plots by the presence of kinks, or deviations, from an otherwise smooth response shape. This is illustrated in the 3(8) mode shape shown in Fig. 6(b). The spline curve fit shows a smooth shape that is characteristic of the 3(8) mode, while the measured FRF data (denoted by solid dots and solid, linear connecting lines) shows a deviation from a purely periodic pattern at blades 10-12.

System Identification

The process described in the previous section was carried out for a number of FRF peaks so that, in conjunction with the deterministic nature of highly-tuned blisk behavior, the response shapes associated with each structural resonance could be identified for the first three families of blade modes. Results are presented in Fig. 7 in which the natural frequencies of the first three blade mode families are plotted versus the number of diametrals in the response shape.

Table 2 summarizes the manner in which data points, associated with the third cantilevered blade-mode family, shown in Fig. 7, were identified. The cells with a single asterisk superscript indicate that the extraction technique summarized in Eqs. (3)-(7) was used to identify the response shapes, cells with a double asterisk superscript indicate that visual inspection of the FRF was used and white cells indicate that the frequencies were linearly interpolated between other, adjacent cells. Note that all modes identified with the extraction technique (single asterisk)

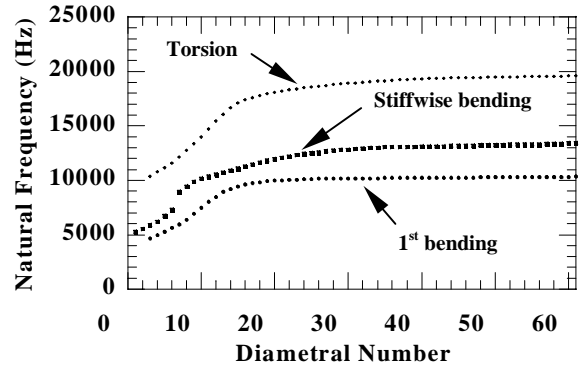


Fig. 7 Blisk natural frequency chart for first three blade-mode families.

were verified using a visual inspection of the FRF (double asterisk). Modes with fewer than three diametrals were not identified for the third blade mode cluster. In order to provide a rigorous determination of the lower-order diametrals, more than 24 blades should be processed in order to obtain a full wavelength around the circumference of the disk. In Fig. 7 and Table 2, however, many of the lower-order blade-mode diametrals, although interspersed with disk modes in the low frequency region, were estimated by extrapolating back in frequency from higher-order, blade-mode diametrals that were obtained with a high degree of confidence. Taken together, Figs. 6-8 represent a summary of the system identification procedure used on the TPA.

Mistuning and Symmetry

The current discussion has treated the blisk as a perfectly tuned system, in which all of the blades are assumed to be identical. In fact, no system is perfectly symmetric, and a small degree of mistuning is, therefore, always present. This slight variability in blade geometry and material properties can admit split resonant peaks at each structural resonance. Specifically, each resonant peak previously identified may, in fact, be one of a pair of two very closely spaced structural resonances that are characterized by the same response shape, albeit with slightly different angular orientations. For the specific case of the blisk, if split resonances were observed for a particular diametral pattern, the average natural frequency of the two is reported in Fig. 7 and Table 2.

In order to provide a general assessment of the degree to which symmetry was present in blade response behavior, a special series of tests were performed. In these tests, the responses at blade number 1 due to impacts at blade numbers 1-5 were compared to the responses at blade number 20 due to impacts at blade

Table 2. Third Blade Mode Natural Frequencies

Diametral Number	Natural Frequency	Diametral Number	Natural Frequency
1	ND	31	18967**
2	ND	32	19014*
3	10377	33	19065**
4	10778	34	19111**
5	11179*	35	19151*
6	11580*	36	19193**
7	12147*	37	19230**
8	12772*	38	19264**
9	13383	39	19299*
10	13994*	40	19329*
11	14708*	41	19355**
12	15425*	42	19386*
13	16064**	43	19397
14	16699**	44	19408
15	17109*	45	19419
16	17390**	46	19430
17	17603*	47	19441
18	17777*	48	19452
19	17934**	49	19463
20	18068**	50	19474
21	18185**	51	19485
22	18300**	52	19496
23	18394**	53	19507
24	18485*	54	19518
25	18572**	55	19529
26	18649**	56	19540
27	18719**	57	19551
28	18789**	58	19562
29	18849**	59	19573
30	18911**	60	19584
		61	19595**

* - Identified with mode extraction technique

** - Identified by inspection of FRF

ND - Not determined

All others linearly interpolated

numbers 20-24. Similarity in the resulting FRFs indicated that a high degree of blade symmetry was present in the blisk response behavior, thus allowing any location (i.e., any stage one blade) to be used as the reference. In the case of the modal identification procedure presented in the previous section, it is, therefore, believed that the approximation of the blisk as a perfectly-tuned system is warranted and provides an accurate approximation of the true system behavior.

Damping Estimates

Damping estimates for stage-one blade response, for each of the three blade mode families, were obtained using the half-power method. PSD functions were used in conjunction with a zero-padding pre-processing step, in which the time histories were padded with an appropriate number of zeroes, in order to obtain finer spectral resolution. As a result, while the original PSD estimates contained a 0.76 Hz resolution that was not deemed sufficient for the half-power method, zero-padding led to an enhanced resolution of 0.11 Hz. The enhanced resolution allowed a series of estimates, for a wide range of resonant peaks in the three blade-mode families, to be obtained. Figure 8 shows the damping estimates (denoted by solid diamonds) for specifically-identified spectral peaks in each of the three blade-mode families. While the damping estimates for each of the three blade-mode families show some variation with frequency, overall magnitudes remain fairly small and do not exceed 0.025% of critical. The relative stability in these estimates, within each blade-mode family, can be taken as an indication of the reasonableness of the half-power method as applied to the enhanced spectral estimates.

It should be understood that using the half-power method to obtain damping values for the blisk is an approximation that relies on the assumption of perfect symmetry and an absence of closely spaced modes, exemplified by the split resonant behavior (inherent in slightly mistuned systems) mentioned in the previous section. The estimates presented in this section were, therefore, checked using more rigorous damping extraction techniques²⁹ that are not discussed herein. The damping estimates obtained from the other methods investigated provided results that confirm the approximations presented in this section.

For the estimates presented in Fig. 8, if double peaks were observed in the FRFs, the data points for the corresponding damping values were higher than those obtained for the single peaks. For example, the 3(25) mode, shown in Fig. 8(c), is shown on a different scale in Fig. 9. Note the double peak in Fig. 9 and the corresponding damping value in Fig. 8(c) that is slightly higher than the rest of the third blade mode cluster. Finally, if any modes associated with higher-order blade clusters were interspersed in the plots intended to show estimates for a lower-order blade cluster, the corresponding damping values were omitted.

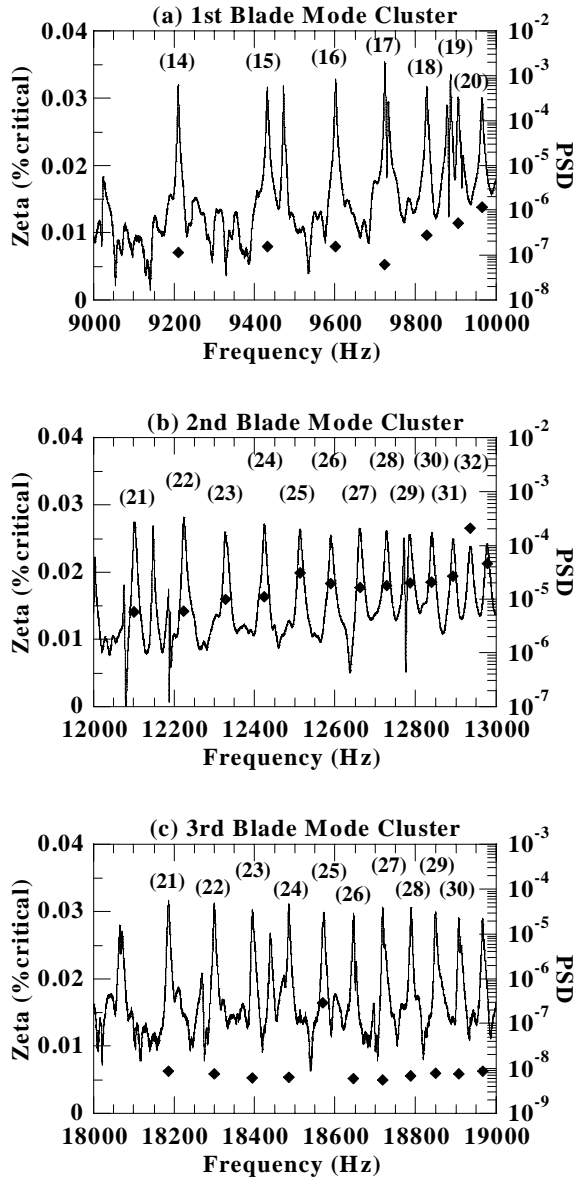


Fig. 8 Damping estimates shown in percent of critical by solid diamonds and referred to the left-hand y-axis for each of the three blade clusters. Solid lines are the PSDs and are referred to the right-hand y-axis. Diametral numbers are shown in parenthesis for the relevant mode clusters.

Conclusions

A method has been proposed to extract modal information from highly-symmetric, lightly-damped bladed disks. The attractiveness of the method lies in its simplicity and the ease in which the results can be interpreted. The method is particularly useful for turbine rotors with short, lightly-damped, stiff blades. In these cases, which require modal identification into

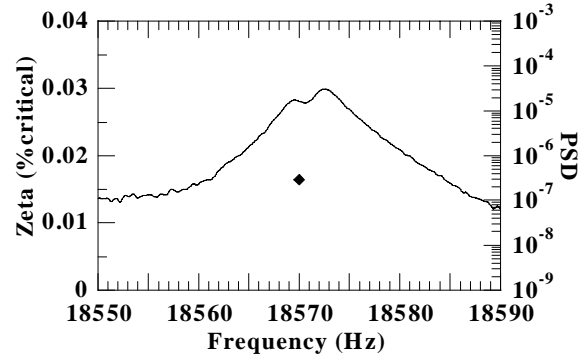


Fig. 9 25th diametral of the third blade mode showing the double peak and its effect on the damping estimate.

the high-frequency regime and, therefore, very high sampling rates and long data records, it is not uncommon that even state-of-the-art data acquisition systems cannot acquire multiple channels of data concurrently. Finally, it is suggested that, compared to more rigorous and established mode-survey-type identification methods, the data required to employ the method described herein can be gathered in significantly less time. While it is acknowledged that the proposed method has certain limitations compared to traditional methods (i.e., orthogonal modes are not extracted), in a compressed schedule the technique can, indeed, help locate potentially harmful resonant conditions in bladed disks and aid in the validation of complex computational models.

Acknowledgments

This work was supported by the U.S. Air Force Materiel Command, Space and Missile Systems Center under Contract F04701-93-C-0094. The authors would like to thank Chafic Hammoud, Myun Kim and Erwin Perl for their contributions to the computational work discussed herein.

References

- ¹Campbell, W., "The Protection of Steam-Turbine Disk Wheels from Axial Vibration," *Spring Meeting of the American Society of Mechanical Engineers*, Cleveland, OH, May 26-29, 1924, 31-160.
- ²Ewins, D., "Vibration Characteristics of Bladed Disc Assemblies," *Journal of Mechanical Engineering Science*, 15(3), 165-186, 1973.
- ³Tobias, S.A. and Arnold, R.N., "The Influence of Dynamical Imperfection on the Vibration of Rotating

Disks,” *Proceedings of the Institution of Mechanical Engineers*, Vol. 171, 1957, 669-690.

⁴Ewins, D.J. and Srinivasan, A.V., *Vibrations of Bladed Disk Assemblies*, The Ninth Biennial Conference on Mechanical Vibration and Noise, Dearborn, Michigan, September 11-14, 1983.

⁵Srinivasan, A.V., *Structural Dynamic Aspects of Bladed Disk Assemblies*, The Winter Annual Meeting of The American Society of Mechanical Engineers, New York, NY, December 5-10, 1976.

⁶Leissa, A.W., MacBain, J.C. and Kielb, R.E., “Vibrations of Twisted Cantilevered Plates – Summary of Previous and Current Studies,” *Journal of Sound and Vibration*, 96(2), 1984, 159-173.

⁷Srinivasan, A.V., “Vibrations of Bladed Disk Assemblies – A Selected Survey,” *Journal of Vibration, Acoustics, Stress, and Reliability in Design*, Vol. 106, April 1984, 165-168.

⁸Duron, Z.H. and DiMaggio, S.J., “High Frequency Impulse Testing of Lightly-Damped Turbine Disks,” Paper No. AIAA-2002-1225, *43rd AIAA/ASME/ASCE/AHS/ASC Structures, Structural Dynamics, and Materials Conference*, Denver, CO, April 22-25, 2002.

⁹Hollkamp, J.J. and Gordon, R.W., “Modal Testing of a Bladed Disk,” *17th International Modal Analysis Conference (IMAC)*, Kissimmee, FL, Feb. 8-11, 1999, 826-832.

¹⁰Lomenzo, R.A., Barker, A.J. and Wicks, A.L., “A Laser Vibrometry System for Rotating Bladed Disks,” *17th International Modal Analysis Conference*, Kissimmee, FL, Feb. 8-11, 1999.

¹¹Fan, Y.C., Ju, M.S. and Tsuei, Y.G., “Experimental Study on Vibration of a Rotating Blade,” *Transactions of the ASME*, Vol. 116, July 1994, 672-677.

¹²Nava, P., Paone, N., Rossi, G.L. and Tomasini, E.P., “Design and Experimental Characterization of a Nonintrusive Measurement System of Rotating Blade Vibration,” *Journal of Engineering for Gas Turbines and Power*, Vol. 116, July 1994, 657-662.

¹³Heath, S., “A Survey of Blade Tip-Timing Measurement Techniques for Turbomachinery Vibration,” *Journal of Engineering for Gas Turbines*, Vol. 120, No. 4, 784-791, 1998.

¹⁴Srinivasan, A.V., Cutts, D.G., and Sridhar, S., “Turbojet Engine Blade Damping,” *NASA Contract Report 165406*, July 1981.

¹⁵Gordon, R.W. and Hollkamp, J.J., “An Internal Damping Treatment for Gas Turbine Blades,” *38th AIAA/ASME/ASCE/AHS/ASC Structures, Structural Dynamics, and Materials Conference & Exhibit*, Kissimmee, FL, April 7-10, 1997, 442-451.

¹⁶Gordon, R.W. and Hollkamp, J.J., “An Experimental Investigation of Non-Uniform Damping in Blade-Disk Assemblies,” *34th AIAA/ASME/SAE/ASEE Joint Propulsion Conference & Exhibit*, Cleveland, OH, July 13-15, 1998.

¹⁷Ahmad, S., Anderson, R.G. and Zienkiewicz, O.C., “Vibration of Thick Curved Shells, with Particular Reference to Turbine Blades,” *Journal of Strain Analysis*, Vol. 5, No. 3, 1970, 200-206.

¹⁸Dokainish, M.A. and Rawtani, S., “Vibration Analysis of Rotating Cantilever Plates,” *International Journal for Numerical Methods in Engineering*, Vol. 3, 233-248, 1979.

¹⁹MacBain, J.C., “Vibratory Behavior of Twisted Cantilevered Plates,” *Journal of Aircraft*, Vol. 12, No. 4, April 1975, 343-349.

²⁰Kielb, R.E., Leissa, A.W. and MacBain, J.C., “Vibrations of Twisted Cantilevered Plates – A Comparison of Theoretical Results,” *International Journal for Numerical Methods in Engineering*, Vol. 21, 1365-1380, 1985.

²¹Srinivasan, A.V., Lionberger, S.R., and Brown, K.W., “Dynamic Analysis of an Assembly of Shrouded Blades Using Component Modes,” *Journal of Mechanical Design*, Vol. 100, 1978, 520-527.

²²Mota Soares, C.A., et al., “Finite Element Analysis of Bladed Disks,” *Structural Dynamic Aspects of Bladed Disk Assemblies*, released at ASME 1976 Winter Annual Meeting, Dec. 5-10, 1976, New York, 73-91.

²³Salama, A.M., et al., “Dynamic Analysis of Bladed Disks by Wave Propagation and Matrix Difference Techniques,” *Structural Dynamic Aspects of Bladed Disk Assemblies*, released at ASME 1976 Winter Annual Meeting, Dec. 5-10, 1976, New York, 45-56.

²⁴Wildheim, J., “Vibrations of Rotating Circumferentially Periodic Structures,” *Quarterly Journal of Me-*

chanics and Applied Mathematics, Vol. XXXIV, Pt. 2, 1981, 213-229.

²⁵Thomas, D.L., "Standing Waves in Rotationally Periodic Structures," *Journal of Sound and Vibration*, 37(2), 1974, 288-290.

²⁶Thomas, D.L., "Dynamics of Rotationally Periodic Structures," *International Journal for Numerical Methods in Engineering*, Vol. 14, 1979, 81-102.

²⁷Afolabi, D., "The Eigenvalue Spectrum of a Mistuned Bladed Disk," *Vibrations of Blades and Bladed Disk Assemblies; Proceedings of the Tenth Biennial Conference on Mechanical Vibration and Noise*, Cincinnati, OH, September 10-13, 1985.

²⁸Wei, S.T. and Pierre, C., "Localization Phenomena in Mistuned Assemblies with Cyclic Symmetry Part 1: Free Vibrations," *Journal of Vibration, Acoustics, Stress, and Reliability in Design*, Vol. 110, October 1988, 429-438.

²⁹Coppolino, R.N., "A Simultaneous Frequency Domain Technique for Estimation of Modal Parameters from Measured Data," *Aerospace Congress & Exposition*, Anaheim, CA, October 5-8, 1981.